The Dickinson Climate Classification: A Taxonomic Thermal-Hydrological Partition of Climate State Space

Caleb Dickinson

Abstract

This paper introduces the Dickinson Climate Classification, a taxonomy that partitions climate state space using evenly spaced thermal metrics and scale-invariant hydrological metrics. Unlike widely used frameworks such as the Köppen classification or the UNEP aridity index, which are calibrated to present-day vegetation distributions or land-degradation objectives, the Dickinson system is formulated as a taxonomic division of climates relevant to the persistence of life. Cold-month and warm-month thermal zones are defined using evenly spaced climatological temperature intervals, while moisture regimes are determined exclusively by dimensionless precipitation-to–potential evapotranspiration (P/PET) ratios and precipitation seasonality metrics, ensuring invariance under uniform rescaling of hydrological fluxes. The resulting framework provides a classification applicable across paleoclimates, present-day conditions, extreme future warming scenarios, and hypothetical climate states. This system is particularly suited for identifying emergent climates with no modern analogues and situating Earth's climates within a broader climate state space.

Document Status and Scope

This manuscript presents a formal climate classification framework. It is not a predictive climate model, attribution study, or impact assessment. The system is intended as a taxonomic and analytical tool for comparing climate regimes across paleoclimates, future warming scenarios, and ecologically relevant climatic states that may never be realized on Earth, without requiring revision of thresholds or category definitions. This manuscript is released as a preprint to establish a persistent, citable description of the Dickinson Climate Classification framework, and is distributed under a

Data and Implementation Notes

All illustrative maps were generated using Google Earth Engine from CHELSA BIOCLIM+ v2.1 1981–2010 climatological normals (Karger et al., 2017; Brun et al., 2022). No new climate model simulations were performed for this work. The classification logic is deterministic and reproducible.

Introduction

The Dickinson Climate Classification differs in both purpose and structure from widely used systems. The Köppen system (Köppen, 1884) is ecological and biogeographic, with classification thresholds calibrated to the present-day distribution of vegetation and climatic analogues on Earth. The UNEP aridity index (UNEP, 1992) is development-oriented, designed primarily to assess land degradation and desertification. In contrast, the Dickinson classification is formulated as an evenly spaced thermodynamic partition of climate state space.

Let $\mathcal{C}_{\text{life}}$ denote the subset of climate state space thermodynamically compatible with the persistence of life. Let $T_{\text{min}}^{\text{life,low}}$ and $T_{\text{min}}^{\text{life,high}}$ denote the lower and upper bounds, respectively, of climatological coldest-month mean temperature compatible with life, and let $T_{\text{max}}^{\text{life,low}}$ and $T_{\text{max}}^{\text{life,high}}$ denote the corresponding bounds for climatological warmest-month mean temperature.

The Dickinson classification is defined only for climates satisfying

$$T_{\text{min}}^{\text{life,low}} \leq T_{\text{min,mean}} \leq T_{\text{min}}^{\text{life,high}}, \qquad T_{\text{max}}^{\text{life,low}} \leq T_{\text{max,mean}} \leq T_{\text{max}}^{\text{life,high}},$$

with the physical constraint $T_{\text{min,mean}} \leq T_{\text{max,mean}}$. These thermodynamic life bounds are not estimated in this work.

Note. Microbial life has been documented in snow at the geographic South Pole (Carpenter et al., 2000), an environment whose climatological monthly mean temperatures correspond to the YY (superarctic with frigid summer) thermal regime in the Dickinson classification. This observation demonstrates that the coldest thermal regime defined in the system occurs within the domain of climates where life can exist.

Biological tolerances are not fixed: they shift over evolutionary time as lineages diverge from

common ancestors and adapt to changing environmental conditions. Systems calibrated to contemporary species distributions therefore embed historical contingency and lose validity when applied to deep-time climates or extreme future scenarios. Thus, classification thresholds in the Dickinson system are evenly spaced instead of species-calibrated.

Millimeter-based precipitation thresholds do not represent equivalent hydrological constraints across climates with different thermal regimes: a fixed precipitation total implies fundamentally different surface water availability in cold versus hot environments due to large differences in evaporative demand. For this reason, aridity regimes in the Dickinson system are defined exclusively using dimensionless ratios of hydrological quantities. No aridity boundary is specified in terms of absolute precipitation totals, absolute evapotranspiration totals, or fixed millimeter thresholds. Instead, aridity classification depends solely on relative water balance and is therefore invariant under uniform rescaling of hydrological fluxes.

The Dickinson classification is intended as a partition of continuous climate space rather than as a definition of habitability limits. It does not attempt to identify the absolute bounds of life. Consequently, hypothetical thermophile-dominated regimes with $T_{\mathrm{max,mean}} = 55°\mathrm{C}$ versus 80°C, for example, may be assigned to the same category. This design choice preserves classification stability across paleoclimatic variability, evolutionary adaptation, and extreme future warming scenarios, without requiring revision in response to newly discovered extremophiles or altered biological tolerances.

Under strong anthropogenic warming, Earth is expected to enter climatic regimes with no present-day analogues, characterized by combinations of thermal and hydrological conditions not historically observed. Classification systems calibrated to modern Earth climate distributions perform well for climates resembling those present at the time of their formulation, but can yield misleading classifications under novel conditions. For example, a hypothetical location with constant rainfall and identical monthly mean temperatures to present-day Phoenix, Arizona would be classified as humid subtropical (Cfa) under Köppen, despite occupying a far more thermodynamically extreme regime than locations such as Tokyo or Atlanta. The Dickinson Climate Classification is designed to address this limitation, providing a framework for tracking climate regime transitions under strong warming, identifying emergent climates with no modern analogues, and comparing paleoclimatic and future states within a single classification scheme.

Additionally, the structure of this system permits higher categorical resolution than most legacy climate classification frameworks, making this classification well suited to resolving sharp climatic gradients, topographic microclimates, and human-relevant thermal regimes.

The system is defined only over the subset of climate space in which the persistence of life is physically possible. Outside this domain, the classification is not meaningful and no interpretation is implied.

Table 1: Conceptual comparison of major climate classification frameworks, including the Dickinson system, the Köppen classification, the Holdridge bioclimatic life-zone scheme (Holdridge, 1947), and the UNEP aridity index.

Classification	**Primary variables**	**Calibration basis**	**Applicability**
Köppen (1884)	Temperature and precipitation thresholds	Observed vegetation distributions	Present-day Earth climates; limited extrapolation
Holdridge (1947)	Biotemperature, precipitation, P/PET	Plant physiological response	Ecological zoning; biologically contingent
UNEP aridity index (1992)	Annual P/PET	Land degradation and desertification risk	Development-oriented; aridity only
Dickinson (this work)	Cold-month $T_{\min}$, warm-month $T_{\max}$, P/PET, seasonality	Thermodynamic partition of climate state space	Paleoclimates, future climates, hypothetical states

1 Thermal Metrics and Cold-Month Thermal Zones

Thermal classification in the Dickinson system is based on climatological monthly mean near-surface air temperatures, computed over a standard 30-year normal period. For each location, the coldest-month mean temperature is taken as the minimum of the twelve climatological monthly means, while the warmest-month mean temperature is taken as the maximum.

The cold-month thermal intervals are defined in uniform increments of 10 °C, with 5 °C resolution used for all but one warm-month category; the *hyperthermal summer* category retains 10 °C spacing. These intervals correspond to simple fractional subdivisions of the 100 °C temperature span between the freezing and boiling points of water at standard pressure. This choice provides a reproducible reference scale without implying special physical thresholds at category boundaries.

The choice of thermal binning reflects a balance between physical interpretability and classification stability, with asymmetric resolution applied to cold- and warm-month metrics. Cold-month thermal zones are defined using uniform 10 °C intervals, as winter tempera-

ture primarily acts as a threshold constraint on surface processes, cryospheric state, and large-scale habitability. Differences smaller than this scale do not typically distinguish fundamentally different winter regimes at the global level, while coarser intervals would collapse thermodynamically distinct cold states.

By contrast, the warm-month thermal axis is partitioned at higher resolution, using 5 °C intervals when a given temperature occurs as a warmest-month mean rather than as a coldest-month mean, across the range of monthly mean temperatures from ≥ 0 to < 40 °C. This reflects the continuous and highly sensitive influence of summer warmth on surface energy balance, evapotranspiration, and heat stress. Accordingly, cold-month thermal classes C, B, A, and Z—defined by their coldest-month means—are each subdivided into paired warm-month categories when their warmest-month means fall within these same numerical temperature intervals (e.g., C into c1 and c2, B into b1 and b2, with analogous subdivisions for A and Z).

This asymmetric treatment follows long-standing precedent in climate classification. In the Köppen system, for example, the temperature spacing between winter-regime isotherms is substantially broader than that separating summer heat regimes (Köppen, 1884). The combined use of uniform 10 °C cold-month bins and finer warm-month subdivisions therefore produces a transparent, scale-consistent partition of climate space that remains robust across paleoclimates, projected future warming scenarios, and hypothetical climate states.

Cold-month thermal zones are assigned using the climatological coldest-month mean temperature ($T_{\mathrm{min,mean}}$), which provides a measure of winter thermal constraint that is insensitive to short-duration extremes. The resulting cold-month thermal zones span the full range of physically plausible climates, from extreme cold environments to hypothetical hyperthermal regimes that may occur under deep-time or future boundary conditions.

Based on $T_{\mathrm{min,mean}}$, climates are assigned to one of the following cold-month thermal zones:

Hypercaneal (H)	$50^{\circ}\mathrm{C} \leq T_{\mathrm{min,mean}} \leq T_{\mathrm{min}}^{\mathrm{life,high}}$
Uninhabitable (X)	$40 \leq T_{\mathrm{min,mean}} < 50^{\circ}\mathrm{C}$
Hyperequatorial (Z)	$30 \leq T_{\mathrm{min,mean}} < 40^{\circ}\mathrm{C}$
Equatorial (A)	$20 \leq T_{\mathrm{min,mean}} < 30^{\circ}\mathrm{C}$
Tropical (B)	$10 \leq T_{\mathrm{min,mean}} < 20^{\circ}\mathrm{C}$
Subtropical (C)	$0 \leq T_{\mathrm{min,mean}} < 10^{\circ}\mathrm{C}$
Temperate (D)	$-10 \leq T_{\mathrm{min,mean}} < 0^{\circ}\mathrm{C}$
Continental (E)	$-20 \leq T_{\mathrm{min,mean}} < -10^{\circ}\mathrm{C}$
Subarctic (F)	$-30 \leq T_{\mathrm{min,mean}} < -20^{\circ}\mathrm{C}$
Arctic (G)	$-40 \leq T_{\mathrm{min,mean}} < -30^{\circ}\mathrm{C}$
Superarctic (Y)	$T_{\mathrm{min}}^{\mathrm{life,low}} \leq T_{\mathrm{min,mean}} < -40^{\circ}\mathrm{C}$

Note on the term "Uninhabitable". *Uninhabitable* denotes climates for which the coldest-month climatological mean temperature satisfies $40^{\circ}\mathrm{C} \leq T_{\mathrm{min,mean}} < 50^{\circ}\mathrm{C}$, implying that all monthly means exceed the core body temperature of humans and other large mammals. The term is thermodynamic in scope and does not preclude habitation by organisms with substantially different size, physiology, or thermal regulation strategies than large mammals, nor technologically mediated habitation.

Note on hypercanes. The term *hypercaneal* is used here strictly as a thermal descriptor for extremely hot climatological monthly mean temperatures. Hypercaneal cold-month and/or warm-month thermal zones should be understood as a *necessary but not sufficient* condition for the formation of hypercane vortices (Emanuel, 1988). Hypercane development also depends on additional dynamical and oceanic factors that are not represented in a monthly-mean thermal classification. Accordingly, classification as hypercaneal does not imply the existence, frequency, or persistence of hypercanes.

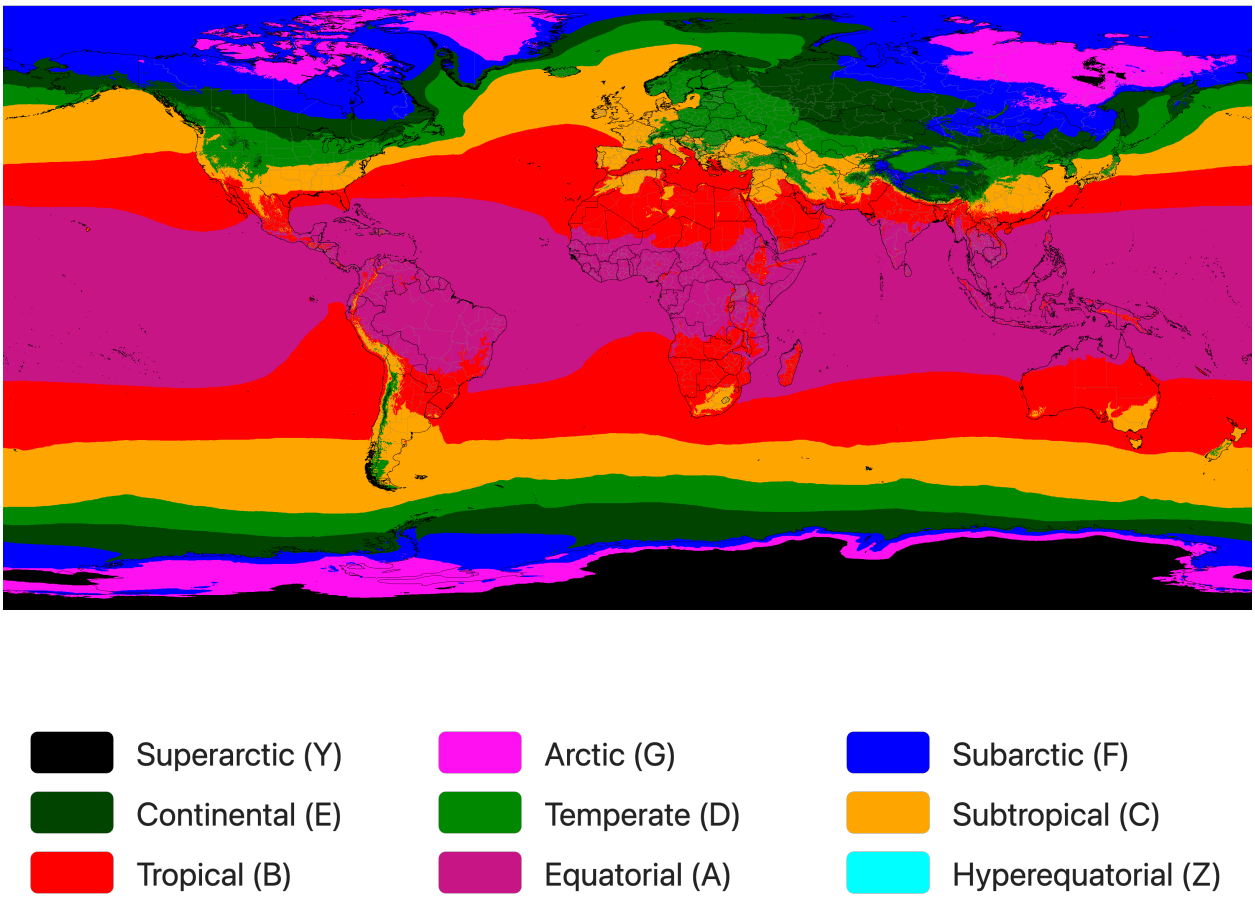

Figure 1: Global distribution of cold-month thermal zones under the Dickinson Climate Classification, based on 1981–2010 climatological normals. Data were processed and plotted in Google Earth Engine (GEE) using CHELSA BIOCLIM+ v2.1 1981–2010 temperature fields (Karger et al., 2017; Brun et al., 2022).

2 Warm-Month Thermal Zones

In addition to cold-season thermal constraints, the Dickinson classification characterizes the intensity of the warm season using the climatological warmest-month mean near-surface air temperature ($T_{\mathrm{max,mean}}$). This metric provides a measure of summer thermal conditions.

Warm-month thermal zones are assigned based on $T_{\mathrm{max,mean}}$ and are intended to distinguish climates with similar winter conditions but substantially different summer heat regimes. The resulting categories span the full range of plausible summer thermal environments, from persistently cold summers to extreme hyperthermal regimes that may occur under deep-time or future warming scenarios.

Based on the warmest-month mean temperature, climates are assigned to one of the following warm-month thermal zones:

Hypercaneal Summer (H)	$50°\mathrm{C} \leq T_{\mathrm{max,mean}} \leq T_{\mathrm{max}}^{\mathrm{life,high}}$
Hyperthermal Summer (X)	$40 \leq T_{\mathrm{max,mean}} < 50°\mathrm{C}$
Scorching Summer (z2)	$35 \leq T_{\mathrm{max,mean}} < 40°\mathrm{C}$
Very Hot Summer (z1)	$30 \leq T_{\mathrm{max,mean}} < 35°\mathrm{C}$
Hot Summer (a2)	$25 \leq T_{\mathrm{max,mean}} < 30°\mathrm{C}$
Warm Summer (a1)	$20 \leq T_{\mathrm{max,mean}} < 25°\mathrm{C}$
Cool Summer (b2)	$15 \leq T_{\mathrm{max,mean}} < 20°\mathrm{C}$
Cold Summer (b1)	$10 \leq T_{\mathrm{max,mean}} < 15°\mathrm{C}$
Very Cold Summer (c2)	$5 \leq T_{\mathrm{max,mean}} < 10°\mathrm{C}$
Freezing Summer (c1)	$0 \leq T_{\mathrm{max,mean}} < 5°\mathrm{C}$
Frigid Summer (Y)	$T_{\mathrm{max}}^{\mathrm{life,low}} \leq T_{\mathrm{max,mean}} < 0°\mathrm{C}$

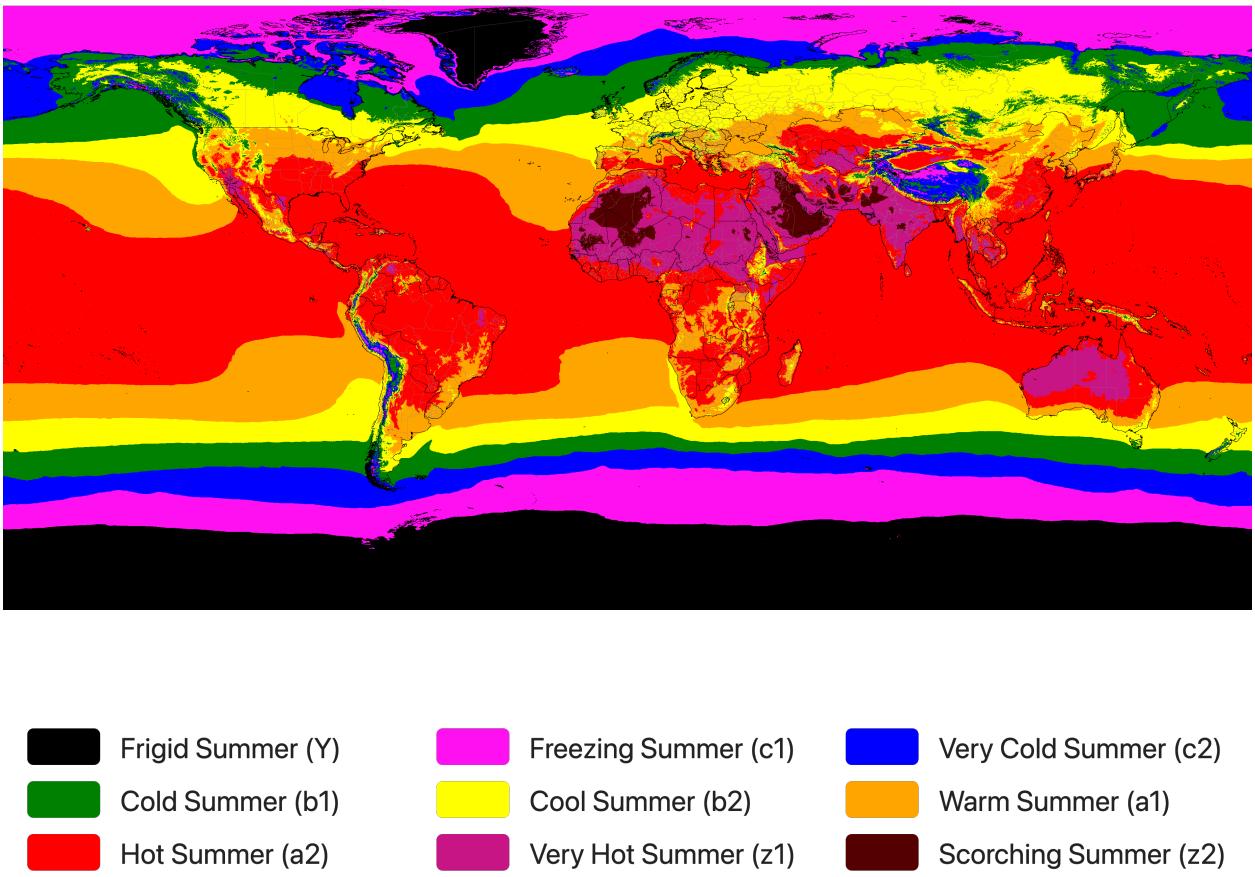

Figure 2: Global distribution of warm-month thermal zones under the Dickinson Climate Classification, based on 1981–2010 climatological normals. Data were processed and plotted in Google Earth Engine (GEE) using CHELSA BIOCLIM+ v2.1 1981–2010 temperature fields (Karger et al., 2017; Brun et al., 2022).

3 Aridity Relevance and Aridity Regimes

Previous climate classification frameworks have implicitly recognized that aridity diagnostics are meaningful only within a limited thermal domain. In the Köppen system (Köppen, 1884), aridity-based categories are restricted to climates whose climatological warmest-month mean temperature exceeds 10 °C, thereby excluding cold-summer and polar regimes in which surface processes are primarily energy-limited rather than moisture-limited. Similarly, the United Nations Environment Programme (UNEP) aridity framework (UNEP, 1992) distinguishes "cold" regions (annual PET $< 400\,\mathrm{mm}$) from aridity regimes defined by P/PET ratios, acknowledging that water-balance diagnostics lose interpretive value where evaporative demand is minimal.

Moisture regime classification in the Dickinson system is applied only to climates in which aridity meaningfully structures surface–atmosphere interactions. Specifically, aridity diagnostics are evaluated only at locations where the warmest-month mean temperature ($T_{\mathrm{max,mean}}$) is at least 15°C and the coldest-month mean temperature ($T_{\mathrm{min,mean}}$) is at least −30°C. Together, these constraints define a conservative thermal envelope within which aridity diagnostics exert first-order influence on climate differentiation. Outside this envelope, climates are classified exclusively on thermal grounds. Consequently, polar, subarctic, alpine, and other climates, such as cold-summer oceanic regimes analogous to Köppen's subpolar oceanic climates, receive no aridity classification within the Dickinson framework.

At locations that do not satisfy these thermal screening criteria, no aridity regime is assigned and the moisture classification is not evaluated within the Dickinson framework. Within this cold thermal regime, aridity diagnostics are not evaluated over either land or ocean. Outside the regime, aridity classification is applied only to terrestrial climates.

For climates meeting the aridity relevance criteria, moisture regimes are defined using the annual aridity index

$$AI = \frac{P_{\mathrm{ann}}}{PET_{\mathrm{ann}}},$$

where annual precipitation is computed as the sum of monthly precipitation totals and where PET denotes annual potential evapotranspiration. All aridity regimes are defined using this dimensionless ratio, ensuring invariance under uniform rescaling of hydrological fluxes.

Based on the annual aridity index, climates are assigned to one of four baseline aridity

regimes in the Dickinson classification:

Humid (h)	$AI \geq 0.75$
Semihumid (g)	$0.50 \leq AI < 0.75$
Semiarid (s)	$0.25 \leq AI < 0.50$
Arid (d)	$AI < 0.25$

For comparison, the United Nations Environment Programme (UNEP) aridity index defines the following regimes:

Humid	$AI \geq 0.65$
Dry subhumid	$0.50 \leq AI < 0.65$
Semi-arid	$0.20 \leq AI < 0.50$
Arid	$0.05 \leq AI < 0.20$
Hyper-arid	$AI < 0.05$

The Dickinson aridity thresholds are modified from the UNEP scheme to provide a more uniform partition of climate space. UNEP's *hyper-arid* and *arid* are incorporated into a single arid category, and each range is repartitioned to produce an aridity index with evenly spaced moisture regimes.

4 Seasonality Diagnostics and Aridity Overrides

In addition to annual water balance, the Dickinson classification incorporates precipitation seasonality diagnostics to distinguish climates with similar aridity indices but fundamentally different seasonal structures. Two complementary diagnostics are used: a high-sun precipitation fraction and a rolling six-month precipitation dominance metric.

The high-sun precipitation fraction (HS) quantifies the proportion of annual precipitation occurring during the six highest-insolation months; April-September in the Northern Hemisphere astronomical extratropics, and October-March in the Southern Hemisphere astronomical extratropics. Annual precipitation during this period (P_{hs}) is divided by total annual precipitation (P_{ann}) to yield

$$HS = \frac{P_{\text{hs}}}{P_{\text{ann}}}.$$

This diagnostic captures hemispherically asymmetric seasonal regimes, particularly extratropical climates characterized by dry summers and wet winters.

To identify strongly concentrated wet seasons independent of calendar alignment, a rolling six-month precipitation dominance metric is also computed. For each possible six-month window, cumulative precipitation is evaluated, and the maximum total ($P6$) is normalized by annual precipitation to yield

$$P6_{\text{ratio}} = \frac{P6}{P_{\text{ann}}}.$$

This metric detects monsoonal regimes in which the majority of annual precipitation occurs within a contiguous portion of the year, regardless of its seasonal timing.

These seasonality diagnostics are applied as overrides to the baseline aridity regimes to distinguish Mediterranean and monsoonal climates.

Mediterranean climates are identified as non-arid regimes ($AI \geq 0.25$) exhibiting strong winter precipitation dominance in the astronomical extratropics ($HS < 0.4$).

Monsoon climates are identified using the rolling six-month precipitation dominance metric. Climates in which at least 80% of annual precipitation occurs within any consecutive six-month period ($P6_{\text{ratio}} \geq 0.8$) are classified as monsoonal, excluding climates already classified as arid or Mediterranean.

Climates meeting the monsoon criterion are classified as *Semiarid Monsoon* when $AI < 0.50$, to distinguish them from monsoon climates with semihumid or humid aridity indices.

Finally, a temperate rainforest override is applied to prevent Mediterranean classification in climates that remain persistently moist throughout the year. For climates initially identified as Mediterranean, the minimum monthly precipitation (P_{driest}) is compared to annual potential evapotranspiration. If

$$P_{\text{driest}} \geq \frac{PET_{\text{ann}}}{24},$$

the climate is reclassified as humid. This criterion corresponds to a minimum monthly precipitation of at least 50% of mean monthly PET.

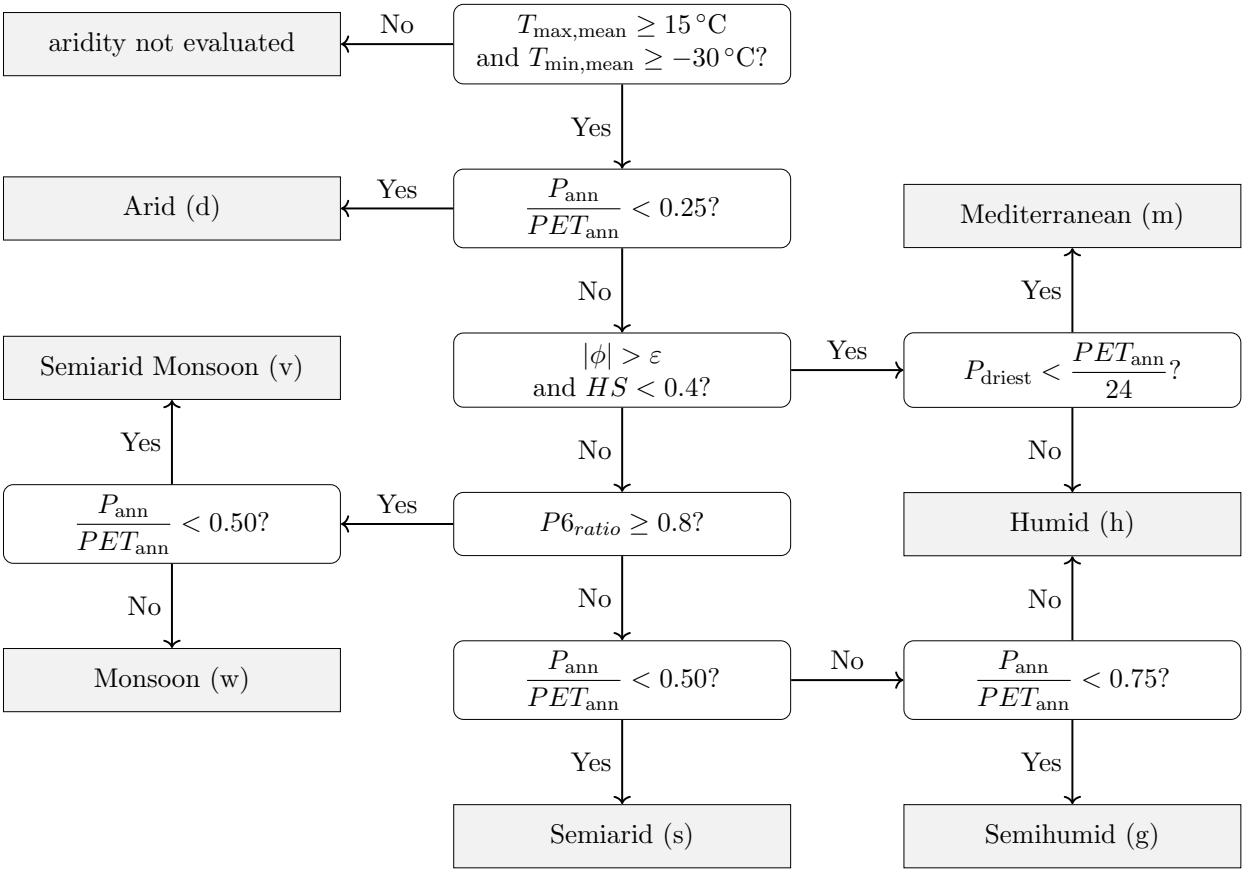

Figure 3: Decision tree for assigning aridity regimes in the Dickinson classification.

Note: ϕ denotes geographic latitude in degrees. ε denotes the Earth's axial tilt (obliquity), defined as the instantaneous angle between the Earth's rotational axis and the normal to its orbital plane. For present-day Earth, $\varepsilon \approx 23.44°$, but ε is treated here as a physical parameter rather than a fixed constant, allowing for secular variation over geological timescales. In this context, extratropical locations are defined as latitudes poleward of the astronomical tropics. Mediterranean seasonality is evaluated only at such locations.

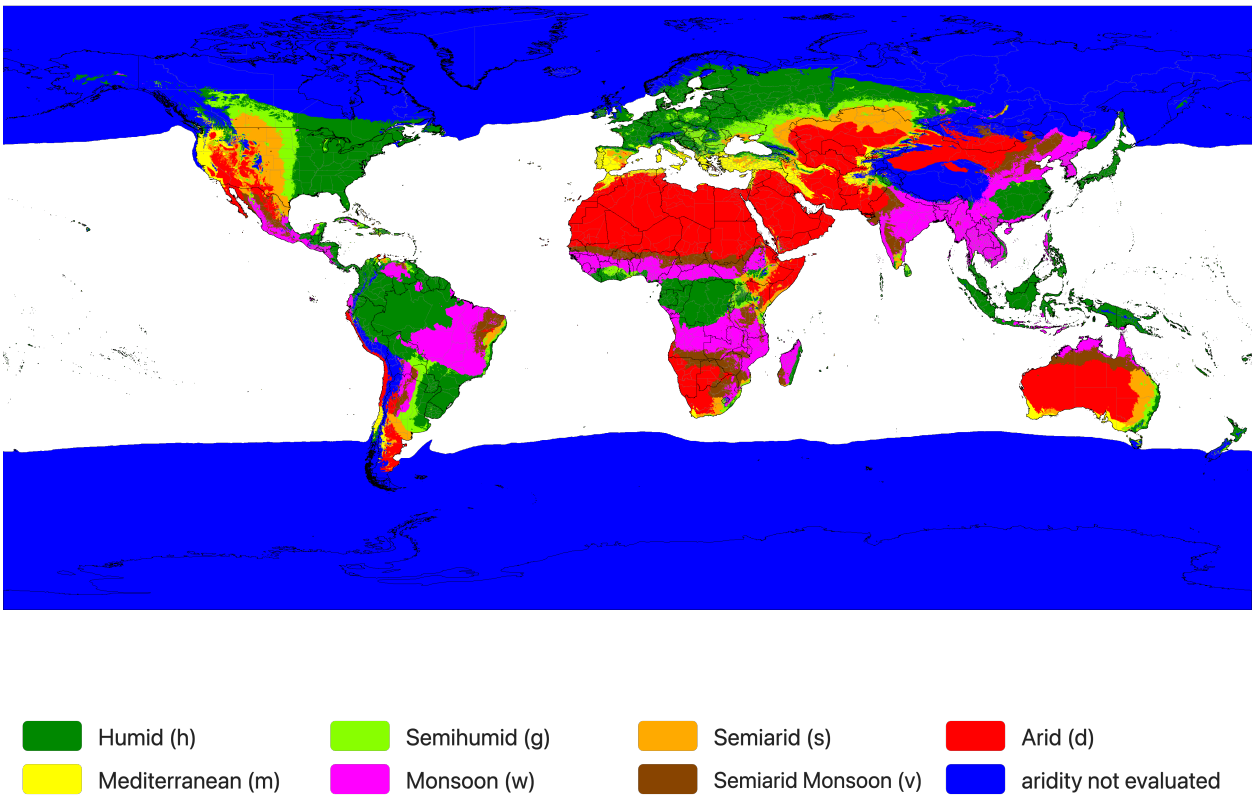

Figure 4: Global distribution of aridity zones under the Dickinson Climate Classification, based on 1981–2010 climatological normals. Data were processed and plotted in Google Earth Engine (GEE) using CHELSA BIOCLIM+ v2.1 1981–2010 precipitation and Penman-Monteith PET fields (Allen et al., 1998; Karger et al., 2017; Brun et al., 2022).

5 Illustrative Climate Codes

The following examples demonstrate the semantic interpretation of Dickinson climate codes. Each code is composed of a cold-month thermal zone, an aridity regime (where applicable), and a warm-month thermal zone, as defined in the preceding sections. These examples are illustrative only and do not necessarily exist on Earth.

- **YY** — Superarctic with frigid summer.
- **Fa2** — Subarctic with hot summer.
- **Ema1** — Continental Mediterranean with warm summer.
- **CdX** — Subtropical arid with hyperthermal summer.
- **Bb1** — Tropical with cold summer.
- **Bhb2** — Tropical humid with cool summer.
- **Zgz2** — Hyperequatorial semihumid with scorching summer.

Conclusion

Climate classification has traditionally been built around the climates that already exist. As the planet warms, that assumption becomes less useful.

The Dickinson Climate Classification treats climate as a state space partitioned using evenly spaced thermal and hydrological metrics. Once that space is defined, climates do not need to resemble anything that exists today in order to be described.

References

Allen, R. G., Pereira, L. S., Raes, D., Smith, M. (1998). Crop evapotranspiration—Guidelines for computing crop water requirements. FAO Irrigation and Drainage Paper No. 56. Rome: Food and Agriculture Organization of the United Nations.

Brun, P., Zimmermann, N. E., Hari, C., Pellissier, L., & Karger, D. N. (2022). Global climate-related predictors at kilometre resolution for the past and future. *Earth System Science Data*, 14, 5573–5603. https://doi.org/10.5194/essd-14-5573-2022

Carpenter, E. J., Lin, S., & Capone, D. G. (2000). Bacterial activity in South Pole snow. *Applied and Environmental Microbiology*, 66(10), 4514–4517. https://doi.org/10.1128/AEM.66.10.4514-4517.2000

Emanuel, K. A. (1988). The maximum intensity of hurricanes. *Journal of the Atmospheric Sciences*, 45(7), 1143–1155. https://doi.org/10.1175/1520-0469(1988)045<1143:TMIOH>2.0.CO;2

Holdridge, L. R. (1947). Determination of world plant formations from simple climatic data. *Science*, 105(2727), 367–368. https://doi.org/10.1126/science.105.2727.367

Karger, D. N., Conrad, O., Böhner, J., Kawohl, T., Kreft, H., Soria-Auza, R. W., Zimmermann, N. E., Linder, P., & Kessler, M. (2017). Climatologies at high resolution for the Earth's land surface areas. *Scientific Data*, 4, 170122. https://doi.org/10.1038/sdata.2017.122

Köppen, W. (1884). Die Wärmezonen der Erde, nach der Dauer der heissen, gemässigten und kalten Zeit und nach der Wirkung der Wärme auf die organische Welt betrachtet. *Meteorologische Zeitschrift*, 1, 215–226.

United Nations Environment Programme. (1992). *World Atlas of Desertification* (2nd ed.). Edward Arnold.